AIAA JOURNAL
Vol. 40, No. 3, March 2002

Neural Network Detection of Shockwaves

Carl Berdahl*
U.S. Air Force Research Laboratory, Wright–Patterson Air Force Base, Ohio 45433

Contemporary neural networks simulate the operation of brain subsystems with substantially higher fidelity than was possible a few years ago. These improvements offer new opportunities to use the cognitive competence of neural networks in fluid mechanics. One such opportunity is developed by taking concepts from their origin in neuroscience through a neural network to the fluid mechanics. The discussion focuses on one brain subsystem (the "What" pathway of the visual system), adapts an existing neural network model of the visual system (the boundary contour system/feature contour system), and shows how a flowfield scalar can excite a pattern of simulated neural activity. The neural network uses three types of shunting neurons found in the retina, lateral geniculate nucleus, and cortical area V1. When shown the density field of a supersonic channel flow, certain neurons in the neural network become active when a shock passes nearby. These active neurons provide a pattern of neural activity that could feed into higher-level What pathway neural networks to make more sophisticated inferences about structures present in a flow. The challenges posed by embedding the current neural network in these higher-level brain structures suggest a promising research agenda.

Introduction

In recent decades there has been a rapid expansion of our knowledge of the mammalian visual system.[1] It is now known that the brain visually identifies objects through the "What" pathway.[2] This pathway begins at the retina, flows to the back of the brain, and then flows downward and forward toward the tip of the temporal lobe (Fig. 1).

Neurons in the What pathway represent more complex features as the visual information flows back through the pathway. A neuron in the retina will fire when a small spot of light falls very close to it.[3] A type of neuron at the back of the brain (cortical area V1) will fire when a small line segment appears in the visual field at a certain location and orientation.[4,5] Near the end of the pathway [inferotemporal cortex (IT)], some neurons fire when the visual system views a face.[6–8]

The What pathway achieves this feature extraction through a kind of mapping from one two-dimensional space to the next, where each two-dimensional space is a sheet of neural tissue. For example, the retina forms the first two-dimensional space in the system.

If one were to unfold the What pathway's U shape, the resulting structure would look, to a first approximation, something like a patchwork quilt with a series of squares of tissue laid end to end (Fig. 2). The lateral geniculate nucleus (LGN), a subcortical structure, is also shown. This mapping resembles a point-to-point mapping, but the mapping from one sheet to the next actually has a small lateral spread due to the axonal arbor at the end of a neuron's axon. Consequently, in V1 (an early stage of the visual system), there exists a tight spatial correspondence between an image on the retina and the neural activity across V1. If an animal viewed a circle on a computer monitor, a special camera looking at the neural activity across cortical area V1 would see approximately the same circle. However, if the same camera looked at cortical area IT (a later stage of the visual system), the camera would see many isolated islands of activity. One could think of each island as one axis in an N space such that the position in this N space codes for the object's identity. This process is sometimes called sparse coding or population coding.[9,10]

Presented as Paper 99-3168 at the 17th Applied Aerodynamics Conference, Norfolk, VA, 28 June–July 1999; received 28 March 2000; revision received 31 August 2001; accepted for publication 4 October 2001.

*Aerospace Engineer, Computational Sciences Branch, Building 146, Room 225, 2210 8th Street.

The preceding account of the feedforward flow of information through the What pathway provides a rough description of the system; additional wiring exists. As Fig. 2 indicates, some information flows backward through the system (feedback pathway). This feedback pathway appears to play an important role in disambiguating incomplete or noisy neural activity in lower level cortex to build a coherent percept.[11,12] Some information also flows laterally between the What pathway and other pathways in the brain. For the current model's needs, though, the feedforward pathway provides sufficient detection power to see shocks.

Computational vision models have duplicated many important aspects of the What pathway. One such model, the boundary contour system/feature contour system (BCS/FCS)[13] contains a neural network model of retinal ganglion cells that respond to spots of light. Other neural network modules within BCS/FCS respond to more complicated shapes such as line segments and T intersections of lines.

Although at first glance it seems unlikely that the feature detection capabilities of a computational vision model would connect in any meaningful way with fluid mechanics, it turns out that one can connect the disciplines by means of the following analogy. The illumination jump across an edge in a scene is like the density jump across a shock in a supersonic flow. Both are step discontinuities of a scalar. The discussion that follows explores this analogy by studying a computational vision model's response when shown the density field of a supersonic channel flow. The current model emulates some of the behavior seen in neurons of the retina, LGN, and cortical area V1. Much of the computational vision model developed in this paper is adapted from the BCS/FCS model.[13] Many concepts used in the BCS/FCS model also appear in the laminar Adaptive Resonance Theory (ART) model,[14] a successor model that implements additional wiring found in cortical areas V1 and V2.

On-Center, Off-Surround Neurons

Construction of the computational vision model begins by describing the behavior of a real on-center, off-surround neuron. This neuron, found primarily in the retina and the LGN, is a kind of workhorse neuron that fires a volley of action potentials in response to a spot of light that falls in the center of its circular receptive field[3] (middle line of Fig. 3). A vertical hashmark denotes an action potential fired by the neuron.

The neuron receives both excitatory input and inhibitory input. Both inputs drive the neuron in a push–pull fashion. Another way of thinking of this is to imagine the accelerator pedal and the brake pedal on a car. Excitatory input presses down on the accelerator pedal, making the neuron fire faster. Inhibitory input presses the brake pedal, slowing the neuron's firing rate. If one pushes down simultaneously on the accelerator pedal and the brake pedal, the

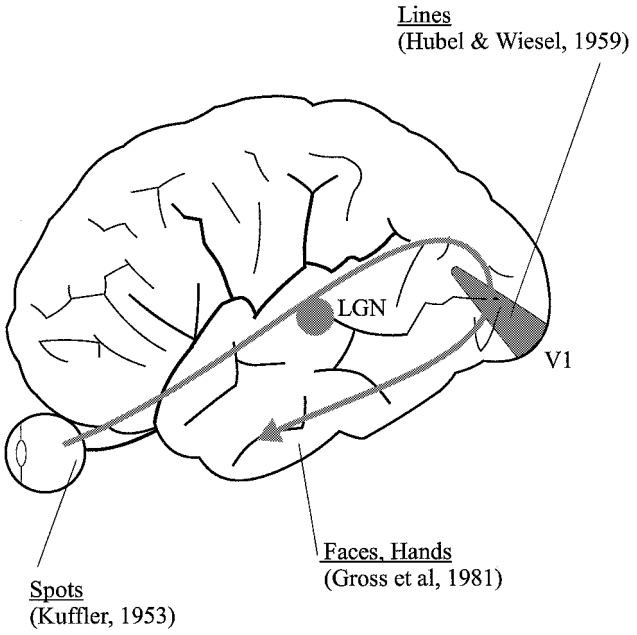

Fig. 1 What pathway.

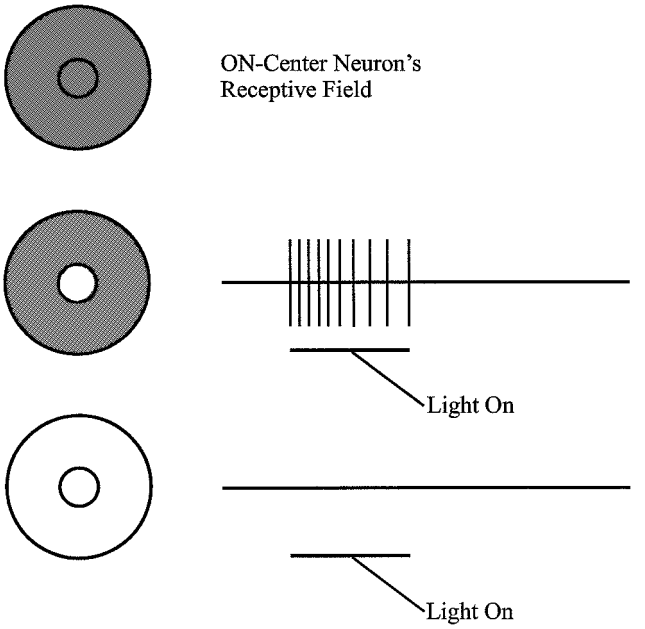

Fig. 3 On-center, off-surround neuron's behavior.

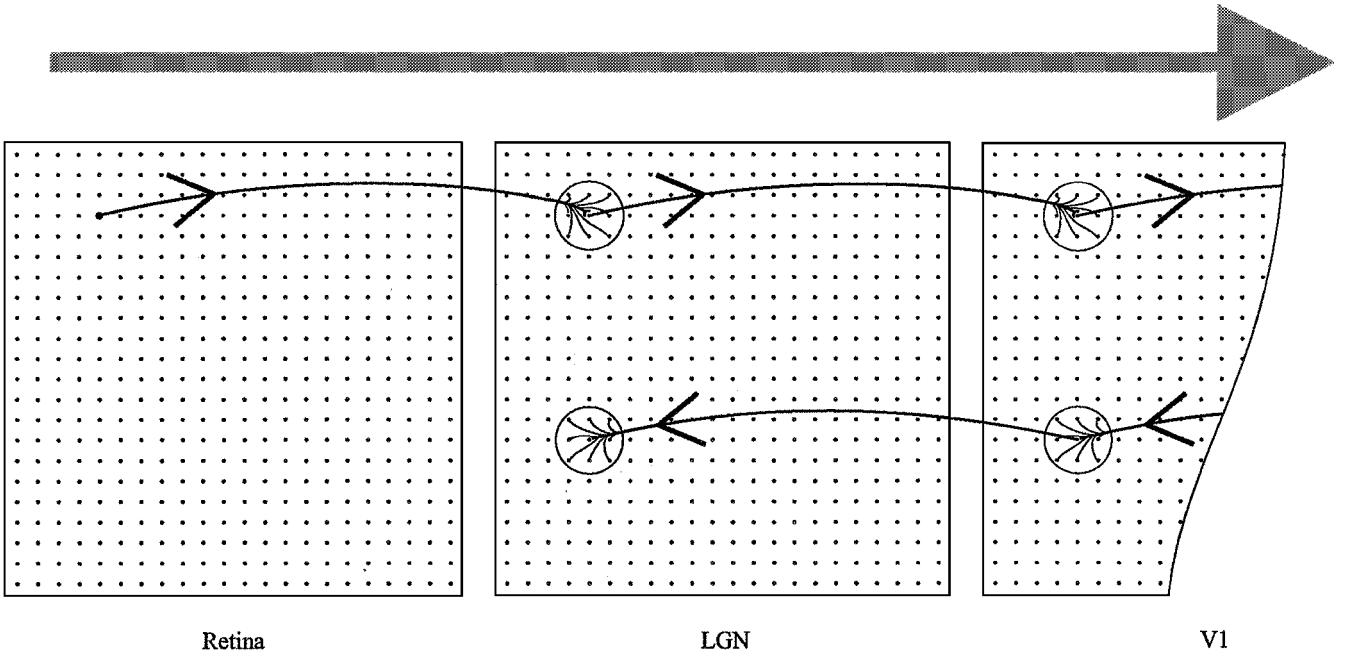

Fig. 2 What pathway mapping.

neuron may settle down at some intermediate firing rate or perhaps not fire at all.

The bottom line of Fig. 3 shows this excitatory–inhibitory balance. In this case, the spot of light has expanded to fill the entire receptive field. Light shining on the off-surround annulus inhibits the neuron such that the inhibition cancels out the excitation, and so the neuron does not fire.

A biological neural network appears to use this excitatory–inhibitory balance as a way to rescale its input so that it will remain responsive even though the overall intensity of illumination may vary over several orders of magnitude. Said another way, this balance gives a neuron a way to see ratios of illumination rather than the overall illumination per se. For example, one edge with 2 lux on the bright side and 1 lux on the dim side would elicit a similar response from a neuron as would an edge with 20 lux on the bright side and 10 lux on the dim side. This similar response occurs even though the differences of illumination across the two edges varies from 1 lux to 10 lux.

Construction of an On-Center, Off-Surround Neuron Model

Figure 4 shows a schematic of an on-center, off-surround neuron. The neuron receives light (illumination) through photoreceptors. The function I describes the illumination profile. The photoreceptors have a higher packing density when the neuron views the light straight on. Only a few photoreceptors report light coming in from the far left and right. The tall, slender Gaussian C in Fig. 5 indicates the packing density.

A Gaussian function [Eq. (1)] expresses the packing density of the C curve (Fig. 5) (also known as a light sensitivity function or an excitatory kernel). The parameters α and μ are constants. The variable r denotes a radius or distance from the center of the Gaussian:

$$C = \alpha e^{-\mu r^2} \tag{1}$$

A convolution integral describes how the neuron gathers light falling on the photoreceptors:

$$\int_{-\infty}^{+\infty} C(r)I(r)\,\mathrm{d}r \tag{2}$$

Relation (2) describes the total excitatory input that the neuron receives. However, as discussed earlier, real neurons receive not only excitation but also inhibition. The inhibition typically comes from a neuron's neighbors (Fig. 6). The inhibitory influence that these neurons have on the current neuron also looks like a Gaussian. This inhibitory Gaussian or kernel (the short, broad E curve in Fig. 5) has a broader lateral spread than the excitatory kernel. The following relation shows how the illumination convolves with the inhibitory kernel E to sum the entire inhibitory input to the neuron:

$$\int_{-\infty}^{+\infty} E(r)I(r)\,\mathrm{d}r \tag{3}$$

The excitatory convolution integral and the inhibitory convolution integral exert their influence on the neuron through a Grossbergian shunting equation[15]:

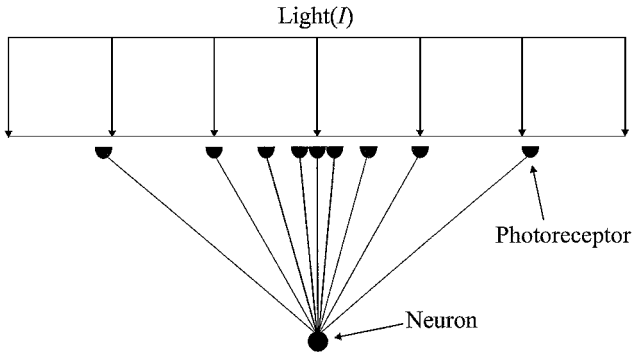

Fig. 4 Neuron schematic.

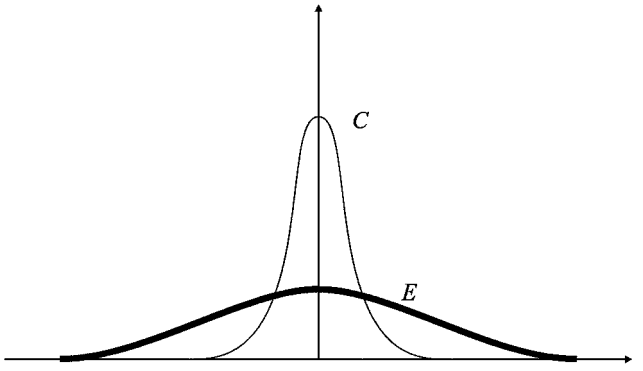

Fig. 5 Overlaid excitatory and inhibitory kernels.

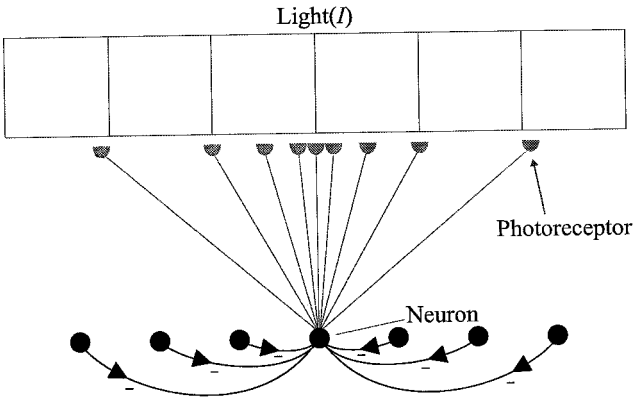

Fig. 6 Inhibitory interactions.

$$\frac{\mathrm{d}x_i}{\mathrm{d}t} = -Ax_i + (B - x_i)\int_A C(A)I(A)\,\mathrm{d}A - (x_i + D)\int_A E(A)I(A)\,\mathrm{d}A \tag{4}$$

The variable x_i is the ith neuron's firing rate. The right-hand side of Eq. (4) contains three terms that control the rate of change of neuronal firing. These terms describe passive decay, excitatory input, and inhibitory input, respectively.

The first term, $-Ax_i$, describes a passive decay. If the other two terms are zero, then the neuron's activity will decay at an exponential rate to zero.

The second term in Eq. (4),

$$(B - x_i)\int_A C(A)I(A)\,\mathrm{d}A$$

describes the excitatory input to the neuron. The convolution integral multiplies the expression $(B - x_i)$. This expression says that excitatory input can push the neuron aggressively when the firing rate x_i is small. However, when x_i becomes large, perhaps almost as large as B, then input can not excite the neuron much further because $(B - x_i)$ is small. This forces the neuron's firing rate to stay below the shunting limit B, just as a real neuron has an upper bound on how fast it can fire.

The third term in Eq. (4),

$$-(x_i + D)\int_A E(A)I(A)\,\mathrm{d}A$$

describes the inhibitory input to the neuron. The parameter D is a hyperpolarization limit that serves a function similar to that of B except that D forms a lower bound on the neuron's firing rate.

To gain some sense of relative height and breadth of the excitatory and inhibitory kernels, Fig. 5 overlays the kernels. Note the broad lateral spread of the inhibitory kernel compared to the excitatory kernel.

Simulated Behavior of an On-Center, Off-Surround Neuron

It is useful to study how a computer-simulated on-center, off-surround neuron responds to two simple illumination fields. Understanding how they respond in these situations will aid in interpreting the neural responses seen later when a field of such neurons views the density field of a supersonic channel flow.

A uniform illumination field offers a convenient place to start. In this case, I is constant. For a steady-state condition, Eq. (4) reduces to $x_i = \text{const}$. This constant may be negative or positive depending on the values chosen for B, D, and the other parameters. A neuron's response in this situation is something like looking at an all-white television screen. Because illumination is everywhere the same, all of the neurons respond at the same rate or, with a suitable choice of parameters, do not respond at all. There are no features on the screen to be seen.

When a step discontinuity in illumination appears, however, the neurons begin to respond in a more sophisticated way. Figure 7

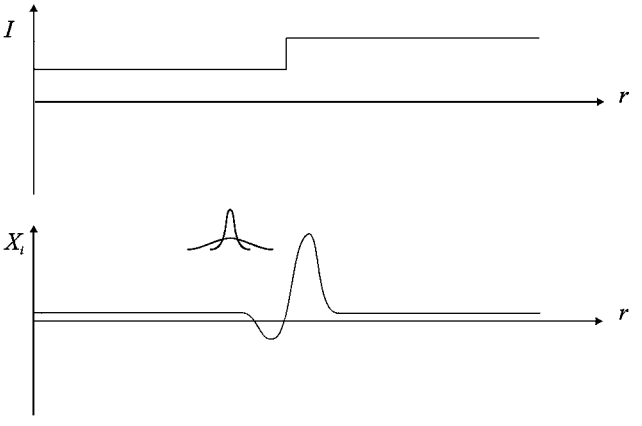

Fig. 7 Neural response to illumination step.

shows the illumination field and one neuron's response. The excitatory and inhibitory kernels appear near the neural response to give a better indication as to why the neuron responds as it does.

As the neuron approaches the illumination step from the left, both the excitatory and inhibitory kernels see only a constant illumination. However, as the neuron moves farther to the right, the right flank of the inhibitory kernel begins to sense the illumination step. Because the excitatory kernel is smaller and does not yet feel the step, inhibition becomes somewhat stronger while the excitatory input to the neuron does not change. The net effect is to inhibit the neuron so that the neuron's activity x_i decreases.

With further movement to the right, however, the excitatory kernel begins to feel the step. Excitation increases, and the neuron's activity x_i increases. This trend continues such that the neuron becomes strongly excited. Eventually, the left portion of the inhibitory kernel also feels the step, and neural activity decreases back to its baseline level.

One other interesting property of this simulated neuron is that it responds primarily to ratios of illumination rather than differences of illumination.[11] As already mentioned, real neurons have a similar property. In a fluid mechanics setting, this property would lead to a similar response from a neuron that viewed the density field of a flow or the same density field normalized by the freestream density.

How a Neuron Sees the Fluid Density in a Computational Fluid Dynamics Grid

Although the preceding discussion explains how to build a computational neuron, showing a neuron the density across a flowfield requires solution of another problem. The density at discrete points in the flowfield must map to the neuron's excitatory and inhibitory kernels. Figure 8 shows the geometry involved for a small section of a computational fluid dynamics (CFD) grid.

The current work solves this mapping problem by curve fitting the 10-term polynomial equation (5) to the local density field. The variables x_1 and x_2 are independent variables that describe a spatial position. The variable x_3 is the dependent variable, which here is the fluid density ρ. The c_i are constants. During the curve-fitting procedure, the algorithm searches for all triangle centroids that fall within the bounds of the kernel (defined here as the radial distance where the Gaussian decreases to 1% of its peak height). The fluid density values at these centroids provide the raw data for the curve fitting:

$$x_3 = c_1 + c_2x_1 + c_3x_1^2 + c_4x_1^3 + c_5x_2 + c_6x_2^2 + c_7x_2^3 + c_8x_1x_2 + c_9x_1x_2^2 + c_{10}x_1^2x_2 \tag{5}$$

Once the polynomial equation curve fits the local density field, a discrete version of the kernel provides a way to compute the convolution integral. The kernel has 32 sections. Radial distances of 0, 20, 50, 80, and 100% of the kernel's boundary delimit the kernel's sections.

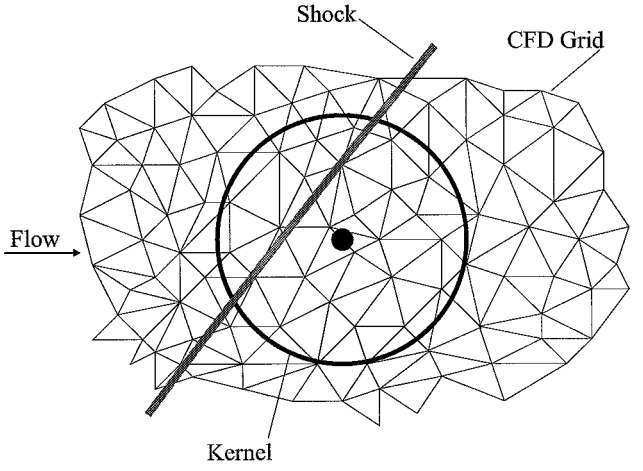

Fig. 8 Two-dimensional kernel superimposed on CFD grid.

The convolution integral in discrete form is relation (6). The height of the kernel and the magnitude of the illumination are both sampled at an area-weighted radius in each sector by inserting the coordinates in Eqs. (1) and (5), respectively,

$$\sum_j C_j I_j A_j \tag{6}$$

On-Center, Off-Surround Neural Response to Supersonic Flow

With the preceding computational model of an on-center, off-surround neuron in hand, the next step was to show an array of these neurons the density field of a supersonic channel flow (Fig. 9). Flow entered the left side of the channel at Mach 1.9. An Euler CFD flow solver[16] computed the flow on an unstructured grid consisting of 4096 triangular cells.

Figure 9 has several major flow features. One oblique shock propagates upward and downstream from the bottom of the channel at the beginning of the ramp. This oblique shock joins a normal shock emanating from the top of the channel and a second oblique shock that propagates downward and to the right. The expansion fan propagates upward and downstream from the top of the ramp. The slip-line originates at the shock–shock intersection. Density increases discontinuously as the flow decelerates through a shock. Density decreases smoothly as the flow accelerates through an expansion fan. Density jumps discontinuously across a slip line but is smeared somewhat here due to numerical diffusion of the CFD flow solver.

An array of on-center, off-surround neurons viewed the density field of this flow. This array comprised a kind of retina. The resulting steady-state neural activity appears in Fig. 10. In Fig. 10, each of the 3346 dots represents a neuron. Larger dots denote more active neurons (large x_i). Neurons with negative x_i are thresholded to zero. The neurons see the shocks fairly well, but a close inspection of Fig. 10 shows that the active neurons fall slightly downstream of the shocks. This slight offset makes sense in light of the behavior of the inhibitory and excitatory kernels relative to an illumination step. Recall Fig. 7 and the neural activity peak set slightly to the high side of the illumination step.

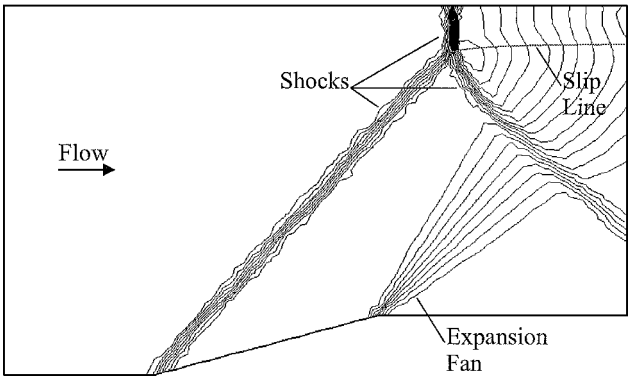

Fig. 9 Density field.

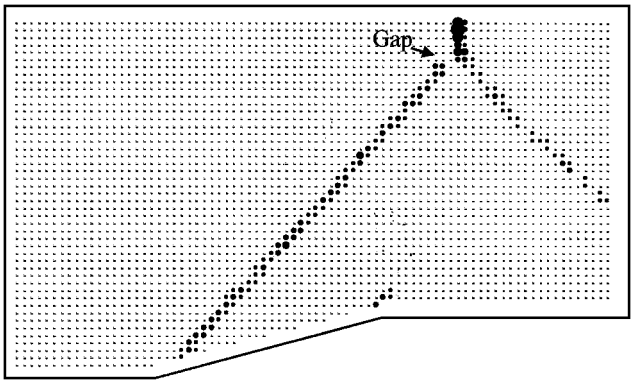

Fig. 10 On-center, off-surround neural activity field.

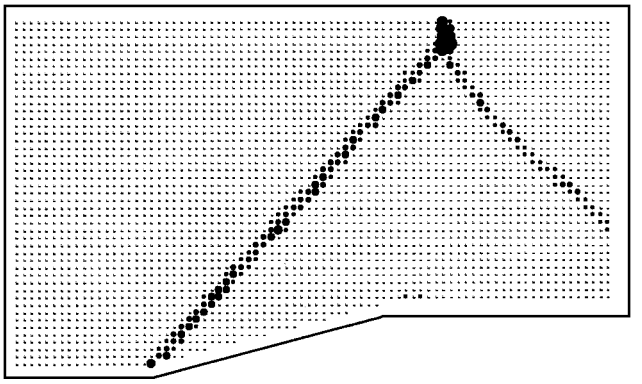

Fig. 11 Off-center, on-surround neural activity field.

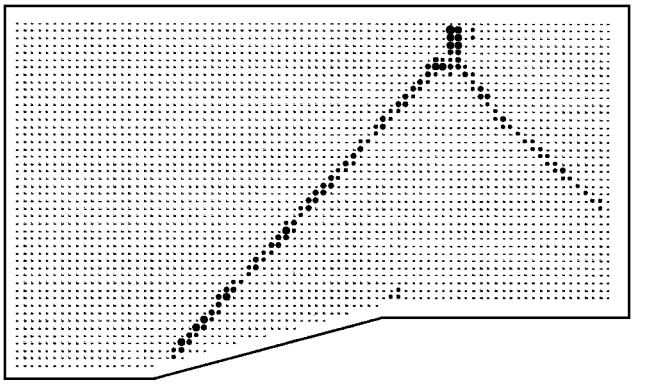

Fig. 12 On/off-neural activity field.

Another curious feature in Fig. 10 is the neural activity gap in the most upstream shock, where it joins the other two shocks. This gap may stem from the fact that the density jumps a large amount across a normal shock but substantially less across an oblique shock. Consequently, the relatively high density on the downstream side of the normal shock exerts a strong inhibitory effect on other neurons in the area. This inhibitory effect may have shut down neurons in the gap, where the small excitatory kernels could not bridge the gap.

Aside from detecting shocks, also note that a few neurons have detected the base of the expansion fan. The density varies across an expansion fan without the step discontinuity characteristic of a shock. Nevertheless, the neurons detect the strong density gradient at the base of the fan. The active neurons fall on the upstream side of the expansion fan.

For coding convenience, no neurons appear around the perimeter of the flowfield. Placing neurons in this area requires special handling with something like ghost cells outside the boundary of the flowfield due to the necessity of searching for density values throughout the entire area covered by the excitatory and inhibitory kernels.

Off-Center, On-Surround Neural Response to Supersonic Flow

As seen in the preceding section, on-center, off-surround neurons become most active on the downstream side of a shock and the upstream side of an expansion fan. Off-center, on-surround neurons behave in the opposite way. They become most active on the upstream side of a shock and the downstream side of an expansion fan. Figure 11 shows the activity of a field of off-center, on-surround neurons that viewed the density field in the channel. As with the on-center neurons, off-center neurons with negative x_i are thresholded to zero.

The following equation shows the shunting equation for the off-center, on-surround neuron:

$$\frac{\mathrm{d}x_i}{\mathrm{d}t} = -Ax_i + (B - x_i)\int_A E(A)I(A)\,\mathrm{d}A - (x_i + D)\int_A C(A)I(A)\,\mathrm{d}A \tag{7}$$

The excitatory and inhibitory convolution integrals have simply switched places from where they were in Eq. (4).

The new broad lateral spread of the excitatory kernel has closed the gap at the shock intersection. This closure demonstrates how a neuron's receptive field size affects what a neuron sees.

On/Off-Neural Response to Supersonic Flow

The preceding sections showed that on-center and off-center neurons can detect shocks in a supersonic flow. However, the active neurons fall on either side of the shocks. To precisely locate the shocks, a third field of neurons is required. These neurons (on/off neurons) would ideally become active only if they sense both active on-center neurons and active off-center neurons. These on/off neurons somewhat resemble complex cells, a type of neuron found in primary visual cortex (V1), in that this cortical area combines different types of neural input in such a way that neurons there respond to somewhat more complex shapes than simple spots of light.[1]

Construction of the on/off shunting equation (8) follows a form similar to Eqs. (4) and (7). However, the input comes now not from the density but from the on and off cell activity in a given neighborhood:

$$\frac{\mathrm{d}x_i}{\mathrm{d}t} = -Ax_i + (B - x_i)\int_A Cx_{\mathrm{ON}}\,\mathrm{d}A\int_A Cx_{\mathrm{OFF}}\,\mathrm{d}A - (x_i + D)\int_A Ex_{\mathrm{ON}}\,\mathrm{d}A\int_A Ex_{\mathrm{OFF}}\,\mathrm{d}A \tag{8}$$

Figure 12 shows a field of on/off neurons as they respond to the neural activity in the on-center and off-center fields. On/off neurons with negative x_i are thresholded to zero. The on/off neurons center the shocks. They also see the base of the expansion fan because of the high-density gradient there. They do not see the slip line because numerical diffusion of the CFD flow solver smears out the density variation across the slip line.

The Appendix provides additional information on the computer simulations.

CFD Grid Adaptation

Figure 12 suggests an intriguing possibility. Neural activity could flag which CFD grid cells need further decomposition so as to resolve the shocks more precisely. Figure 8 indicates how this might be done. The neuron in Fig. 8 appears as a black dot in the middle of the kernel. If this neuron were an on/off neuron and were active, an algorithm could simply search for the CFD grid cell (triangle) whose centroid lay closest to this active neuron. Once identified, a variety of algorithms could decompose (chop up) the grid cell in a suitable way for a CFD flow solver. With smaller grid cells here, the flow solver could more precisely locate the shock after running a few hundred more iterations on the new grid.

Neural activity could also guide a reduction in CFD grid density. Inactive neurons over certain portions of the flowfield where the density did not change significantly could flag these grid cells as unnecessarily small. An algorithm could combine several small grid cells into one larger grid cell. The resulting reduction in number of grid cells would free up computational resources for use elsewhere, that is, resolving shocks.

Although other adaptive grid algorithms exist, the author believes that the current work describes the first use of a computational vision neural network model that could guide grid adaptation to a flow feature. The ability of the current neural network to see the shocks represents a low-level form of intelligence (simple feature detection) inspired by biological neural networks. The incorporation of this form of intelligence sets the current approach apart from other adaptive grid algorithms. Note that the intelligence in the current neural network stems from its imitation of real biological neural networks and differs fundamentally from the artificial intelligence (AI) approaches that seek to reduce intelligence to a set of if–then (rule-based) decisions.

Future Work

A network of on-center, off-center, and on/off neurons forms a convenient foundation for follow-on work that engages higher levels of the visual system. As mentioned in the Introduction, neurons in higher-level visual cortex respond to more complex shapes such as faces and hands. Much as in the real visual system, a more sophisticated model could use the current network's activity as input to the higher levels. These higher levels could then, in turn, make inferences about what flow features appeared in a scene. In this case, instead of becoming active when presented with a face, a population of neurons would become active when presented with a vortex or separation bubble, for example. Once recognized, the grid cells in these areas could be refined to resolve the flow more precisely.

Although the current work shows how neural network detection of a flow feature could aid CFD grid adaptation, it is plausible that a neural network could find operational applications, as well. In principle, if one had good real-time information about some scalar in a supersonic channel flow, a neural network could detect the presence of certain flow features, for example, shocks, and manipulate a control device such as a ramp, boundary-layer bleed, fluid injection, and so forth to force the flow into some desirable state. A motor control neural network such as the vector associative map (VAM)[17] could perhaps use input from a sensory neural network to learn autonomously how to manipulate a control device.

Extension of the network to handle a three-dimensional flow provides a more near-term research goal. This would require a three-dimensional retina, something that has no parallel in biology. However, no obvious impediment exists to extending the neural network in this way. The kernels would simply sense density in three dimensions instead of two dimensions.

Finally, the approach presented could conceivably find application in other disciplines. For example, the finite element decomposition of a structure might use a neural network to identify stress concentrations in the structure and, thereby, modify the decomposition to better capture these stresses.

Conclusions

Advances in neural network modeling of brain subsystems offer new opportunities to use brain modeling concepts in fluid mechanics. This paper presents one example of how to develop such an opportunity by briefly describing the brain's What pathway, adapting an existing neural network model of the early stages of this pathway, and showing this neural network the density field of a supersonic channel flow. Active neurons mark the location of shocks and even detect a small portion of an expansion fan. Embedding the current neural network in higher-level portions of the What pathway should permit detection of more complex flow structures. Challenges posed by engaging these higher-level brain structures suggest a promising research agenda.

Appendix: Neural Network Parameters

The following provides additional information on the computer simulations.

Equation (4) Parameters (on-cells):

$$A = 0.1, \qquad B = 1.265, \qquad D = 0.2$$

The Gaussian [relation (1)] for the excitatory convolution integral [relation (2)] used the following parameters:

$$\alpha = 2.0, \qquad \beta = 50.0$$

The Gaussian [relation (1)] for the inhibitory convolution integral [relation (3)] used the following parameters:

$$\alpha = 12.649, \qquad \beta = 5.0$$

Equation (7) parameters (off-cells):

$$A = 0.1, \qquad B = 0.03162, \qquad D = 0.2$$

The Gaussian [relation (1)] for the excitatory convolution integral used the following parameters:

$$\alpha = 12.649, \qquad \beta = 5.0$$

The Gaussian [relation (1)] for the inhibitory convolution integral used the following parameters:

$$\alpha = 2.0, \qquad \beta = 50.0$$

Equation (8) parameters (on/off cells):

$$A = 0.1, \qquad B = 1.5, \qquad D = 0.2$$

The Gaussian [relation (1)] for both excitatory convolution integrals used the following parameters:

$$\alpha = 50.0, \qquad \beta = 10.0$$

The Gaussian [relation (1)] for both inhibitory convolution integrals used the following parameters:

$$\alpha = 50.0, \qquad \beta = 5.0$$

For coding convenience, the computation of excitatory input to the on/off cell activity did not use a discrete circular neighborhood, but instead sampled a 5×5 array of on-cell and off-cell activity centered over a given on/off cell. The inhibitory input to a given on/off cell sampled a 7×7 array of on-cell and off-cell activity.

Acknowledgment

William Strang of the U.S. Air Force Research Laboratory provided the computed supersonic channel flow.

References

[1] Kandel, E. R., Schwartz, J. H., and Jessell, T. M., *Principles of Neural Science*, 4th ed., McGraw–Hill, New York, 2000, pp. 492–571.

[2] Ungerleider, L. G., and Mishkin, M., "Two Cortical Visual Systems," *Analysis of Visual Behavior*, edited D. J. Ingle, M. A. Goodale, and R. J. W. Mansfield, MIT Press, Cambridge, MA, 1982, pp. 549–586.

[3] Kuffler, S. W., "Discharge Patterns and Functional Organization of Mammalian Retina," *Journal of Neurophysiology*, Vol. 16, No. 1, 1953, pp. 37–68.

[4] Hubel, D. H., and Wiesel, T. N., "Receptive Fields of Single Neurones in the Cat's Striate Cortex," *Journal of Physiology*, Vol. 148, No. 3, 1959, pp. 574–591.

[5] Hubel, D. H., and Wiesel, T. N., "Receptive Fields, Binocular Interaction and Functional Architecture in the Cat's Visual Cortex," *Journal of Physiology*, Vol. 160, No. 1, 1962, pp. 106–154.

[6] Gross, C. G., Bruce, C. J., Desimone, R., Fleming, J., and Gattass, R., "Cortical Visual Areas of the Temporal Lobe. Three Areas in the Macaque," *Multiple Visual Areas*, edited by C. Woolsey, Vol. 1, Humana Press, Totowa, NJ, 1981, pp. 187–216.

[7] Tanaka, K., "Neuronal Mechanisms of Object Recognition," *Science*, Vol. 262, No. 5134, 1993, pp. 685–688.

[8] Wang, G., Tanaka, K., and Tanifuji, M., "Optical Imaging of Functional Organization in the Monkey Inferotemporal Cortex," *Science*, Vol. 272, No. 5268, 1996, pp. 1665–1668.

[9] Young, M. P., and Yamane, S., "Sparse Population Coding of Faces in the Inferotemporal Cortex," *Science*, Vol. 256, No. 5061, 1992, pp. 1327–1331.

[10] Georgopoulos, A. P., Lurito, J. T., Petrides, M., Schwartz, A. B., and Massey, J. T., "Mental Rotation of the Neuronal Population Vector," *Science*, Vol. 243, No. 4888, 1989, pp. 234–236.

[11] Grossberg, S., "How Does a Brain Build a Cognitive Code?," *Psychological Review*, Vol. 87, No. 1, 1980, pp. 1–51; reprint *Studies of Mind and Brain*, D. Reidel, Dordrecht, The Netherlands, 1982, pp. 2–52.

[12] Mumford, D., "On the Computational Architecture of the Neocortex: II The Role of Cortico-cortical Loops," *Biological Cybernetics*, Vol. 66, No. 3, 1992, pp. 241–251.

[13] Grossberg, S., and Mingolla, E., "Neural Dynamics of Perceptual Grouping: Textures, Boundaries, and Emergent Segmentations," *Perception and Psychophysics*, Vol. 38, No. 2, 1985, pp. 141–171.

[14] Ross, W. D., Grossberg, S., and Mingolla, E., "Visual Cortical Mechanisms of Perceptual Grouping: Interacting Layers, Networks, Columns, and Maps," *Neural Networks*, Vol. 13, No. 6, 2000, pp. 571–588.

[15] Grossberg, S., "Contour Enhancement, Short Term Memory, and Constancies in Reverberating Neural Networks," *Studies in Applied Mathematics*, Vol. 52, No. 3, 1973, pp. 213–257.

[16] Grismer, M. J., Strang, W. Z., Tomaro, R. F., and Witzeman, F. C., "Cobalt: A Parallel, Implicit, Unstructured Euler/Navier–Stokes Solver," *Advances in Engineering Software*, Vol. 29, No.3–6, 1998, pp. 365–373.

[17] Gaudiano, P., and Grossberg, S., "Vector Associative Maps: Unsupervised Real-Time Error-Based Learning and Control of Movement Trajectories," *Neural Networks*, Vol. 4, No. 2, 1991, pp. 147–183.

M. Sichel
Associate Editor